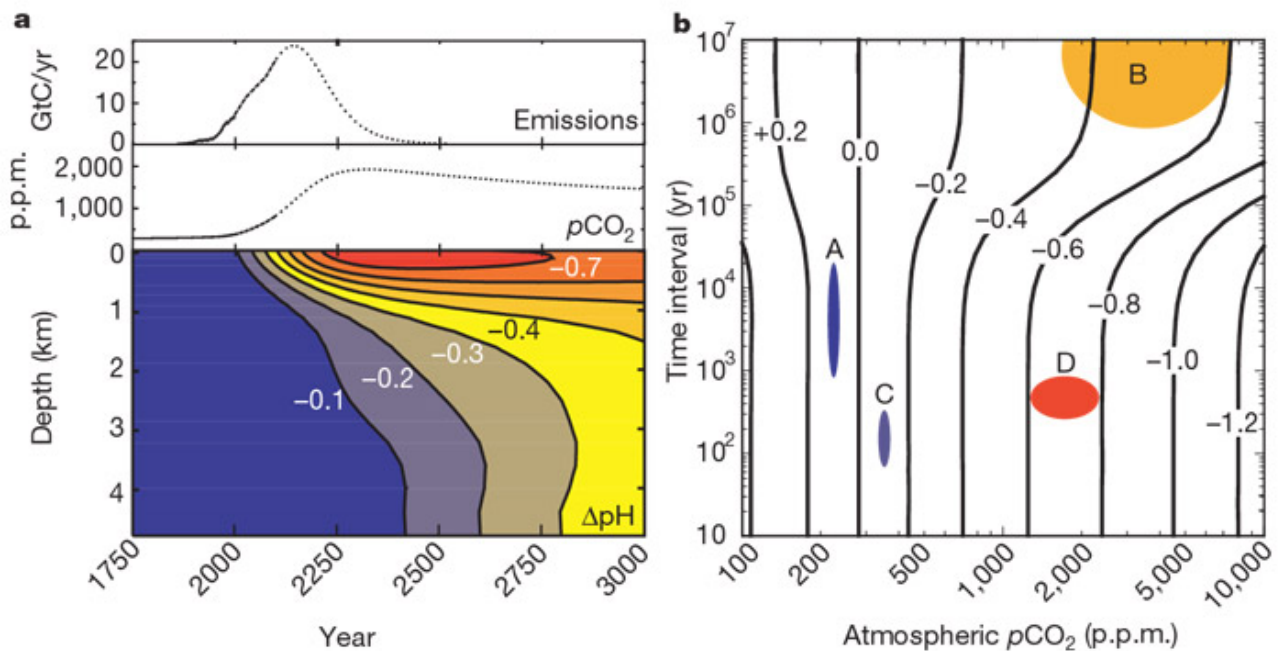
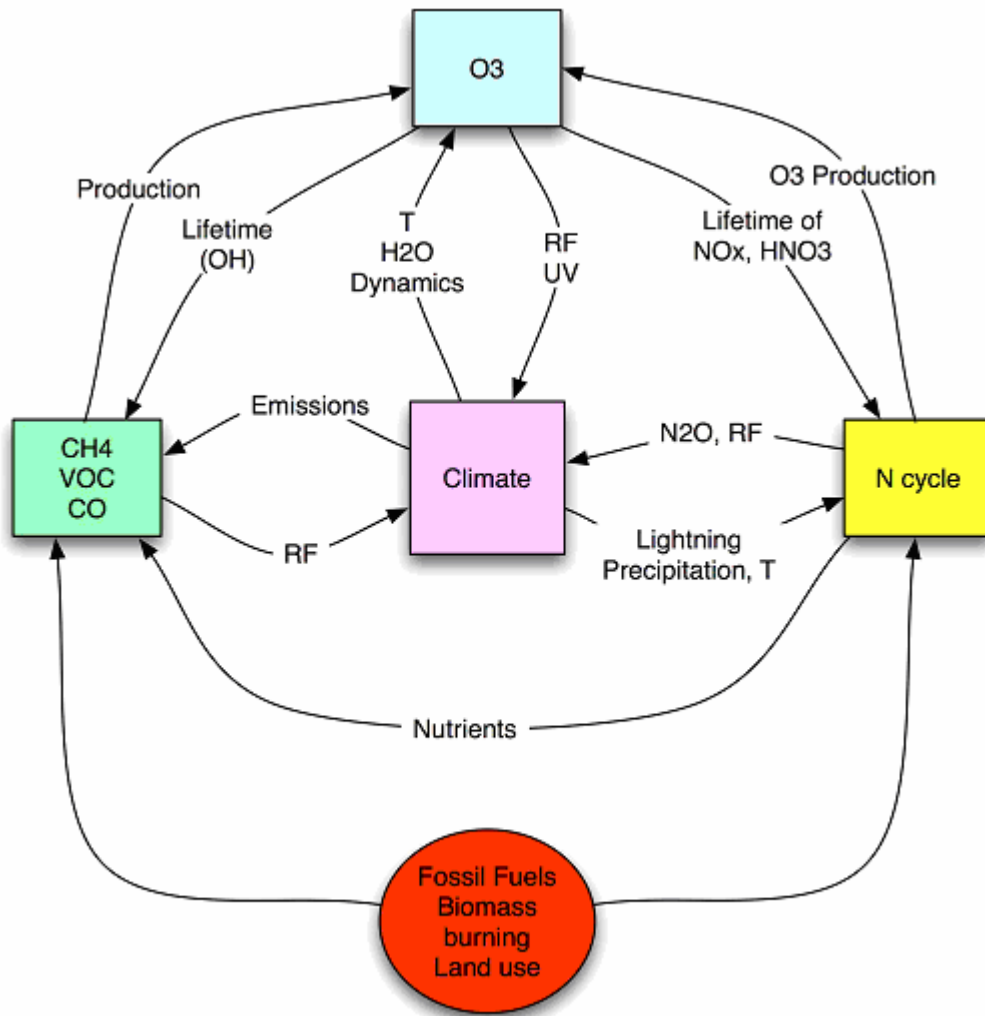


1
23
4
5
6
7
8
9
10
11
12
13
14
15
16

Box 7.3, Figure 1. Atmospheric release of CO_2 from the burning of fossil fuels may give rise to a marked increase in ocean acidity. Panel a: Atmospheric CO_2 emissions, historical atmospheric CO_2 levels and predicted CO_2 concentrations from this emissions scenario, together with changes in ocean pH based on horizontally averaged chemistry. The emission scenario is based on the mid-range IS92a emission scenario (solid line) assuming that emissions continue until fossil fuel reserves decline. Panel b: Estimated maximum change in surface ocean pH as a function of final atmospheric CO_2 pressure, and the transition time over which this CO_2 pressure is linearly approached from $280 \mu\text{atm}$. A. Glacial-interglacial changes; B. slow changes over the past 300 million years; C. historical changes in ocean surface waters; D. unabated fossil-fuel burning over the next few centuries. According to the given emission scenario, oceanic absorption of CO_2 from fossil fuels may result in larger pH changes over the next several centuries than any inferred from the geological record of the past 300 million years. Source: Caldeira and Wickett (2003).

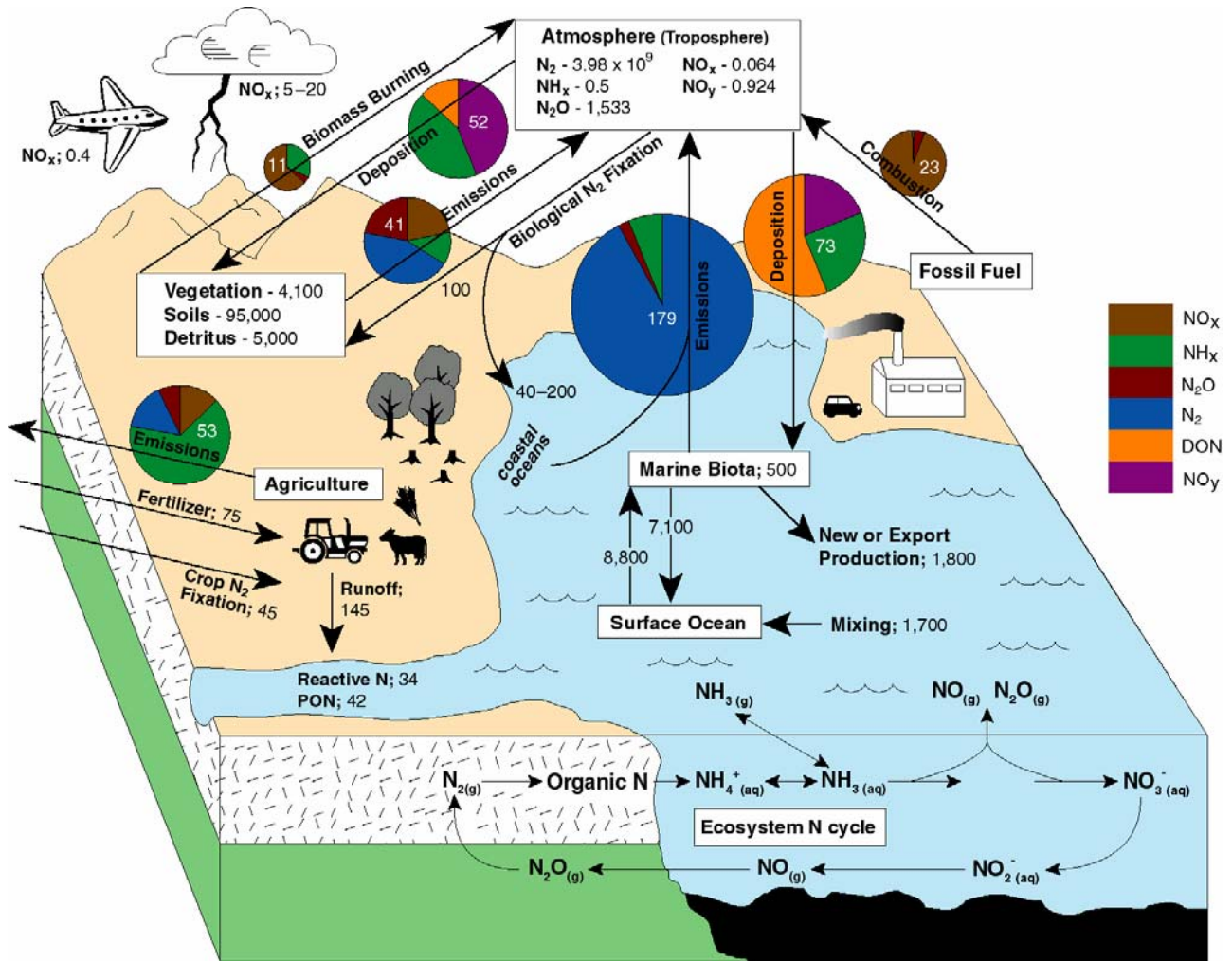
1
2



3
4
5
6
7
8

Figure 7.4.1. Schematic representation of the multiple interactions between tropospheric chemical processes, biogeochemical cycles and the climate system. *RF* represents radiative forcing, *UV* ultraviolet radiation, and *T* temperature.

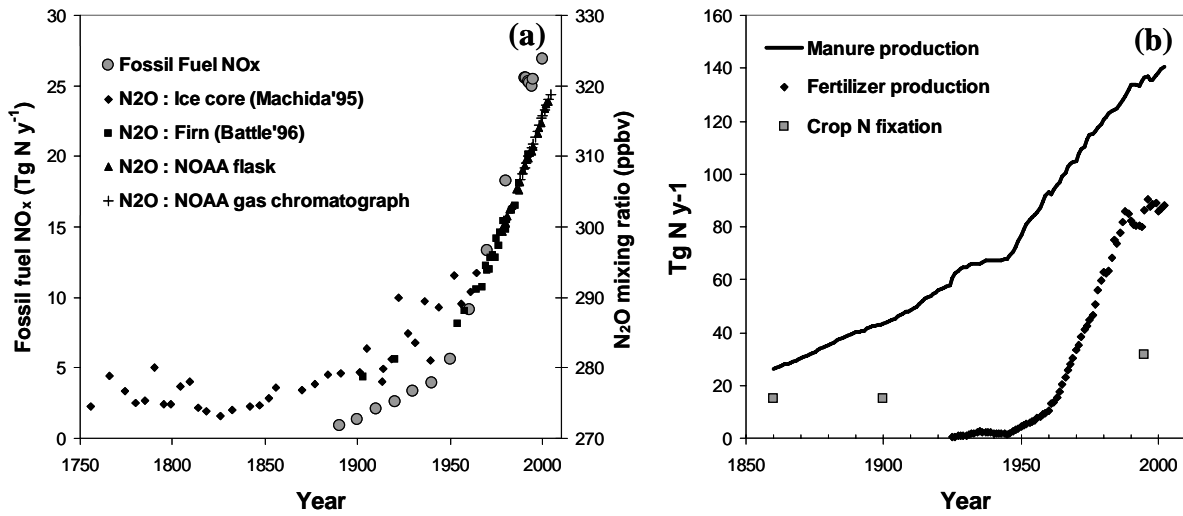
1
2



3
4
5
6
7
8
9
10
11

Figure 7.4.2. Key fluxes and components of the global nitrogen cycle, including emissions and deposition. Each of the key atmospheric species including NO_x ($NO + NO_2$), NH_x ($NH_3 + NH_4^+$), N_2O , N_2 , DON (Dissolved Organic Nitrogen) and NO_y (total odd nitrogen = $NO_x + HNO_3 + HONO + HO_2NO_2 + NO_3 +$ nitrate radical + Peroxyacetyl nitrates + N_2O_5 + organic nitrates) and their fluxes are shown. The ecosystem nitrogen cycle depicts the internal transformations nitrogen going starting with N_2 , and the transformation, nitrification and denitrification, back to N_2 to complete the full cycle. All units are in Tg of N, Tg = 10^{12} g.

1
2



3
4
5
6
7
8
9
10

Figure 7.4.3. (a) Changes in the emissions of fossil fuel NO_x and atmospheric N₂O mixing ratios since 1750. N₂O mixing ratios provide the atmospheric measurement constraint on global changes to the nitrogen cycle. (b) Changes in the indices of global agricultural nitrogen cycle since 1850: the production of manure, fertilizer and estimates of crop nitrogen fixation. For data sources see <http://www-eosdis.ornl.gov/> and <http://www.cmdl.noaa.gov/>.

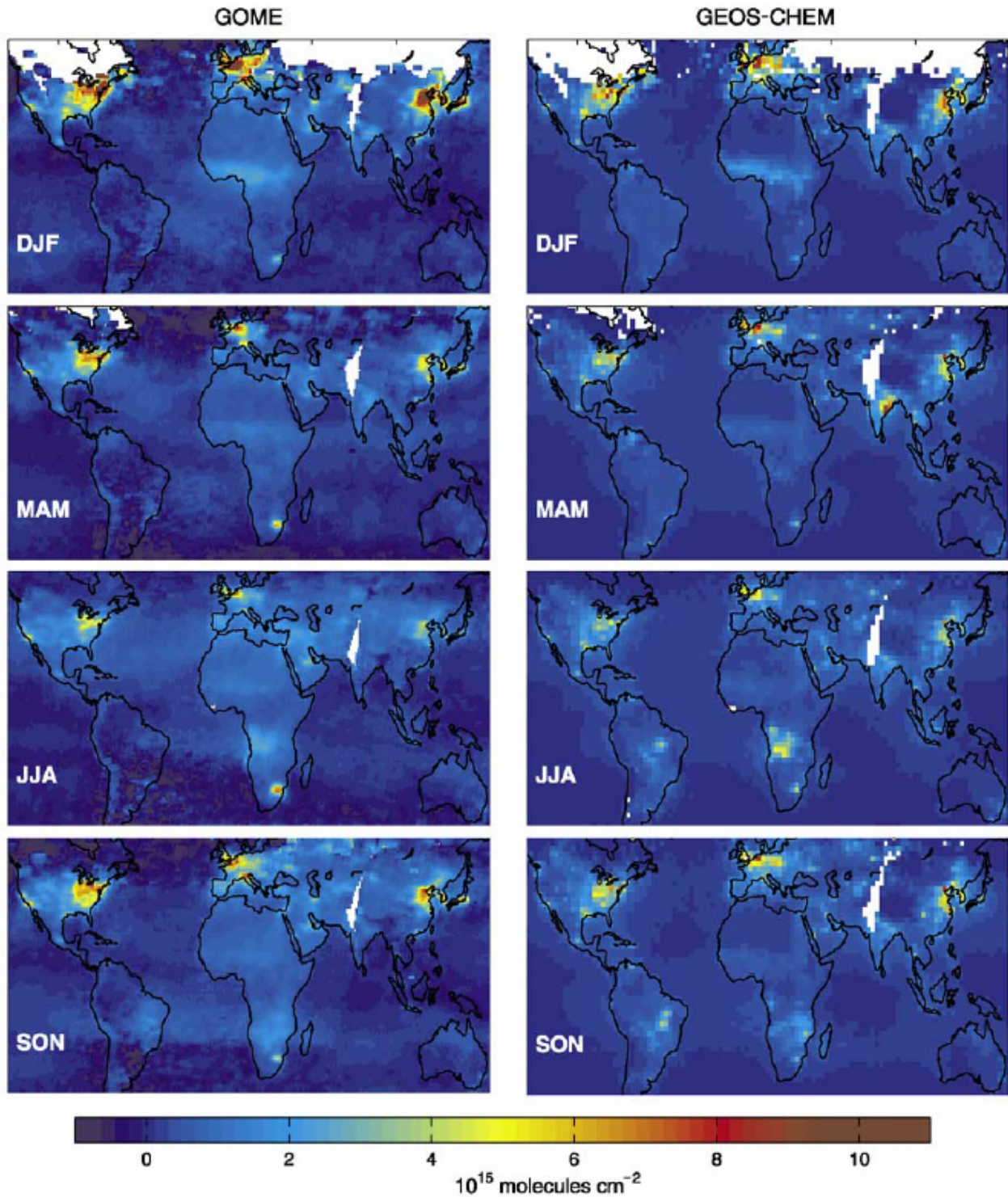
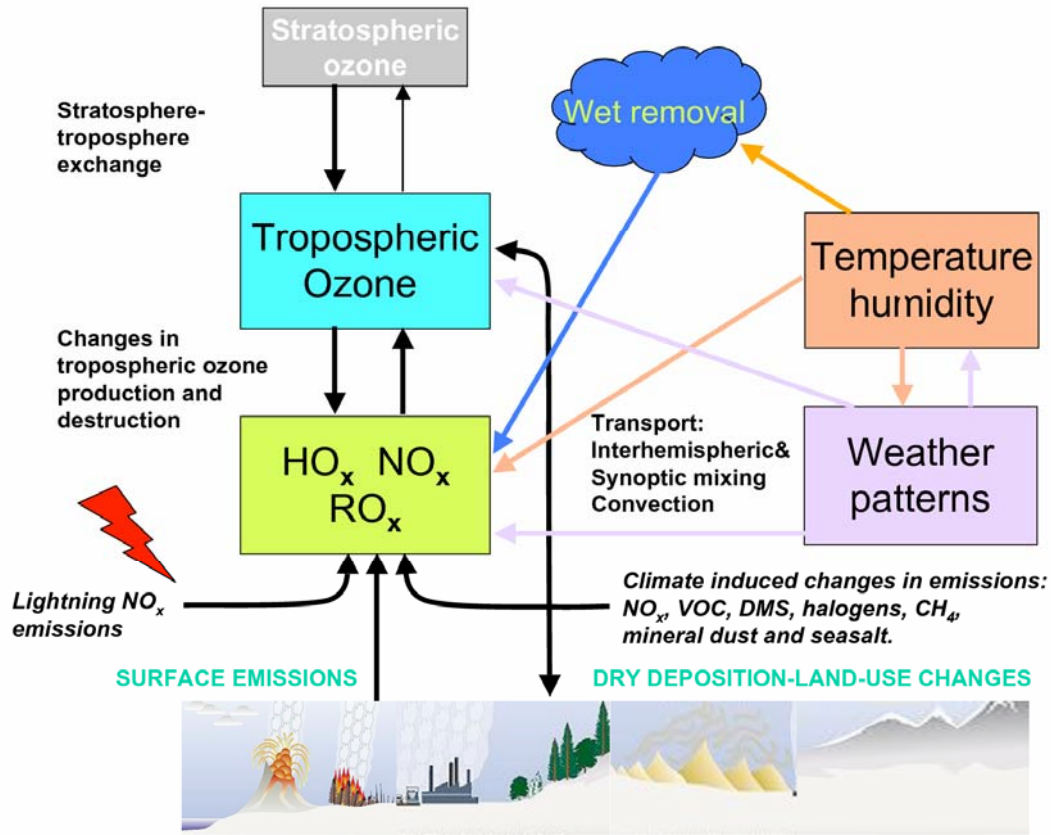
1
23
4
5
6
7
8

Figure 7.4.4. Seasonal mean tropospheric NO₂ columns for September 1996–August 1997. Left: GOME retrievals. Right: GEOS-CHEM model simulation sampled along GOME overpasses and using sources from Table 7.4.4 (Bey et al., 2001). White areas have no GOME data. From Martin et al. (2003b).

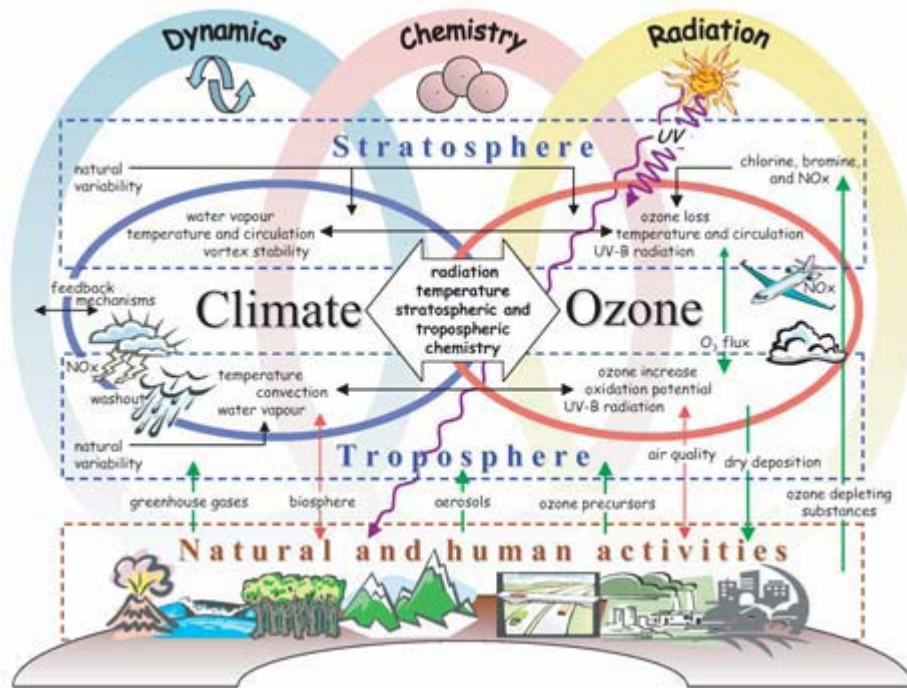
1
2



3
4
5
6

Figure 7.4.5. Climate variables affecting tropospheric ozone. From European Commission (2003).

1
2



3
4
5
6
7
8
9

Figure 7.4.6. Processes determining the ozone climate interactions in the troposphere and the stratosphere (European Commission, 2003). Atmospheric regions are indicated by blue, and source regions by brown dashed boxes.

1
2

3
4

5
6
7
8
9
10
11
12

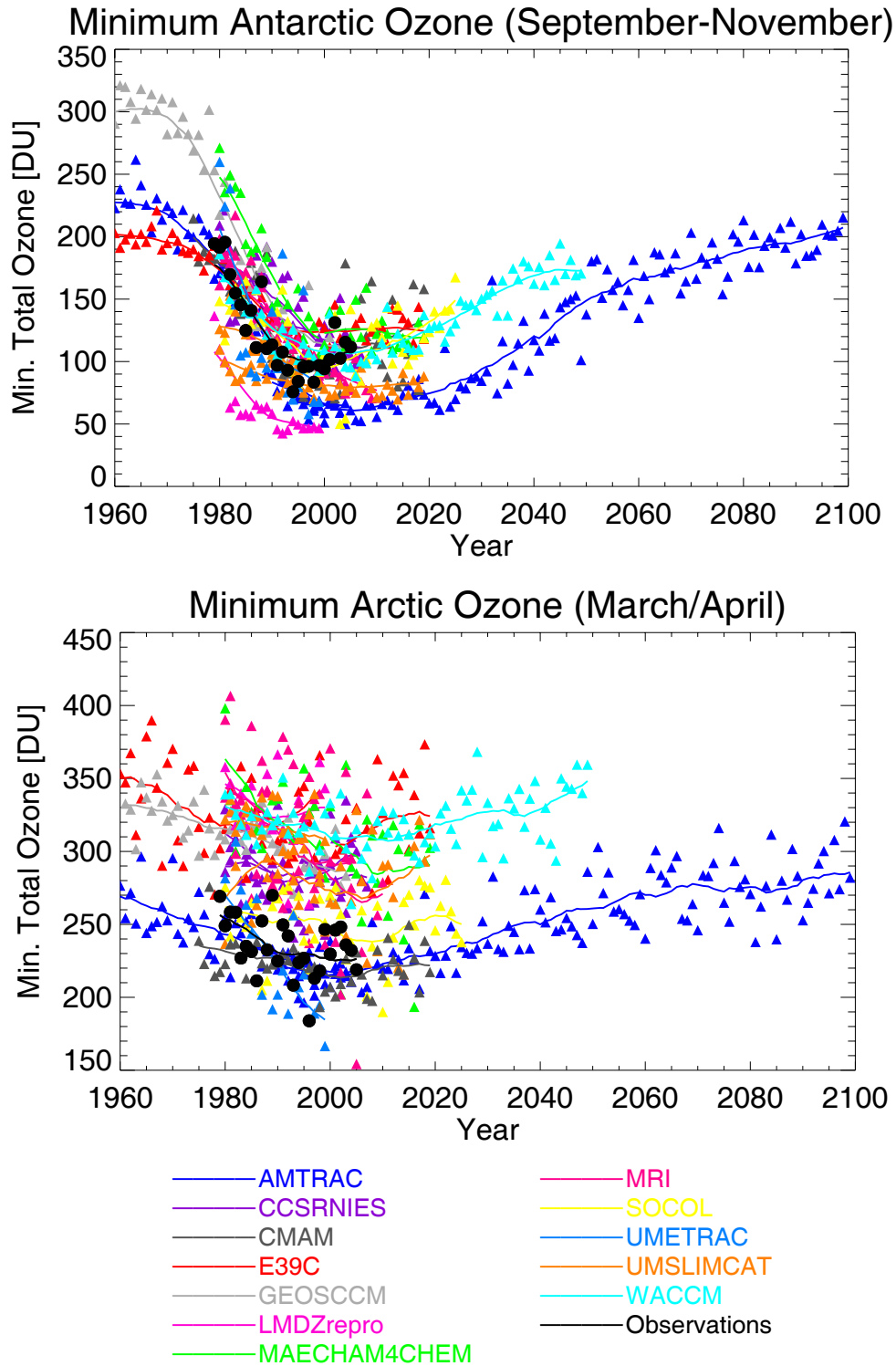
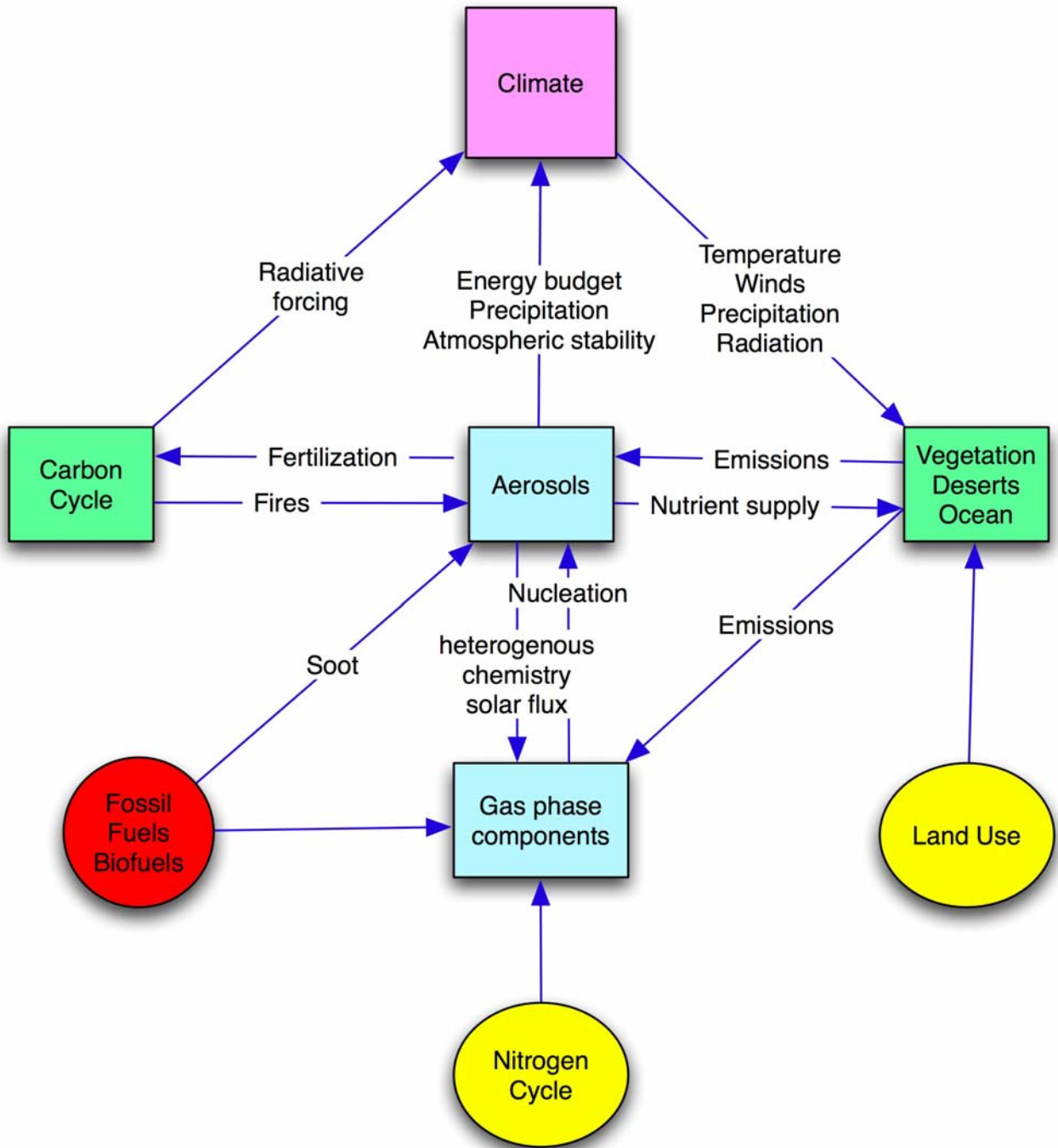


Figure 7.4.7. (a) Minimum Antarctic total ozone for September to November (upper panel) and (b) minimum Arctic total ozone for March to April (lower panel) for various transient coupled chemistry-climate simulations. Model results are compared with the NIWA assimilated data base (Bodeker et al., 2005).

1
2

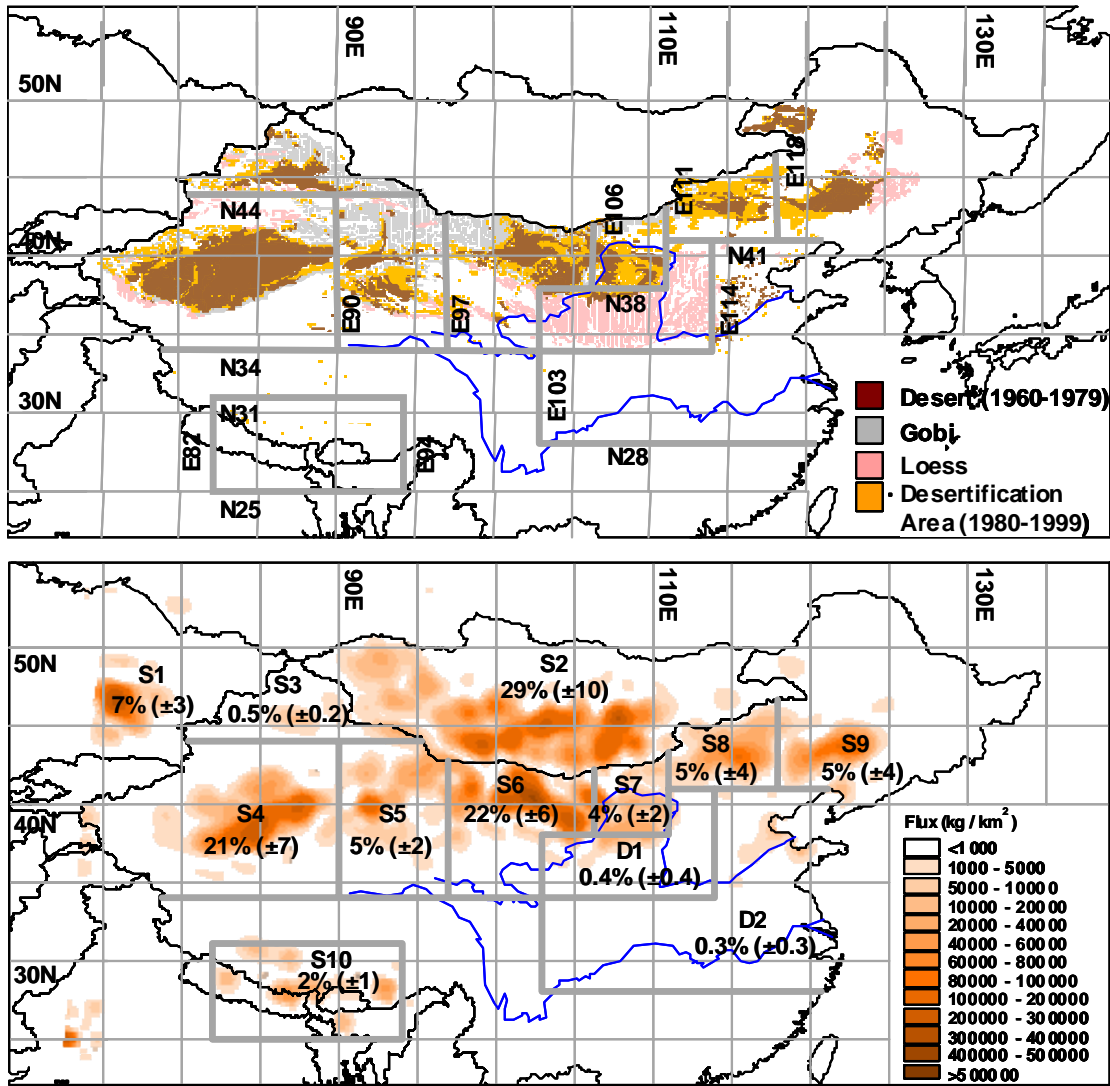


3
4
5
6
7

Figure 7.5.1. Schematic illustrating the interactions of aerosols with the climate, the carbon cycle, gas-phase chemistry, deserts and the marine and continental biosphere.

1
2

3

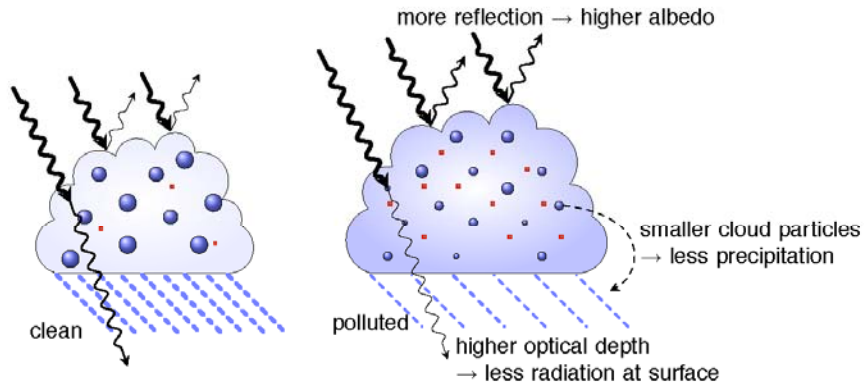


4
5
6
7
8
9
10
11
12
13
14

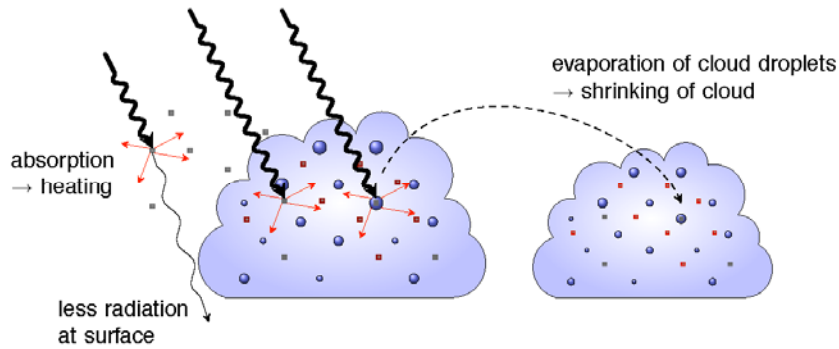
Figure 7.5.2. (a) Chinese desert distributions from 1960–1979 and desert plus desertification areas from 1980–1999; (b) Sources (S1 to S10) and typical depositional areas (D1 and D2) for Asian dust indicated by spring average dust emission flux ($\text{kg km}^{-2} \text{ month}^{-1}$) between 1960–2002. The percentages with standard deviation in the parenthesis denote the average amount of dust production in each source region and the total amount of emissions between 1960–2002. The deserts in Mongolia (S2) and in western (S4) and northern (S6) China (mainly the Taklimakan and Badain Juran, respectively) can be considered as the major sources for Asian dust emissions. Several areas with more expansions of deserts (S7, S8, S9 and S5) are not key sources. Adapted from Zhang et al. (2003).

1
2

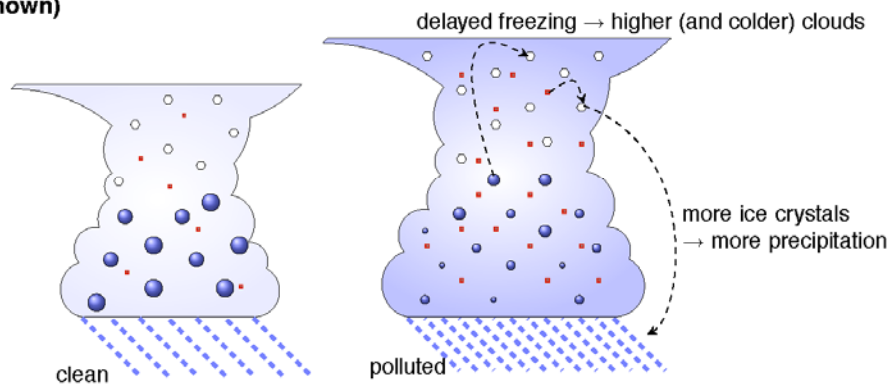
Cloud albedo and lifetime (negative radiative effect for warm clouds at TOA and less precipitation); solar dimming (less radiation at the surface)



Semi-direct effect (positive radiative effect at TOA for soot inside clouds, negative for soot above clouds)



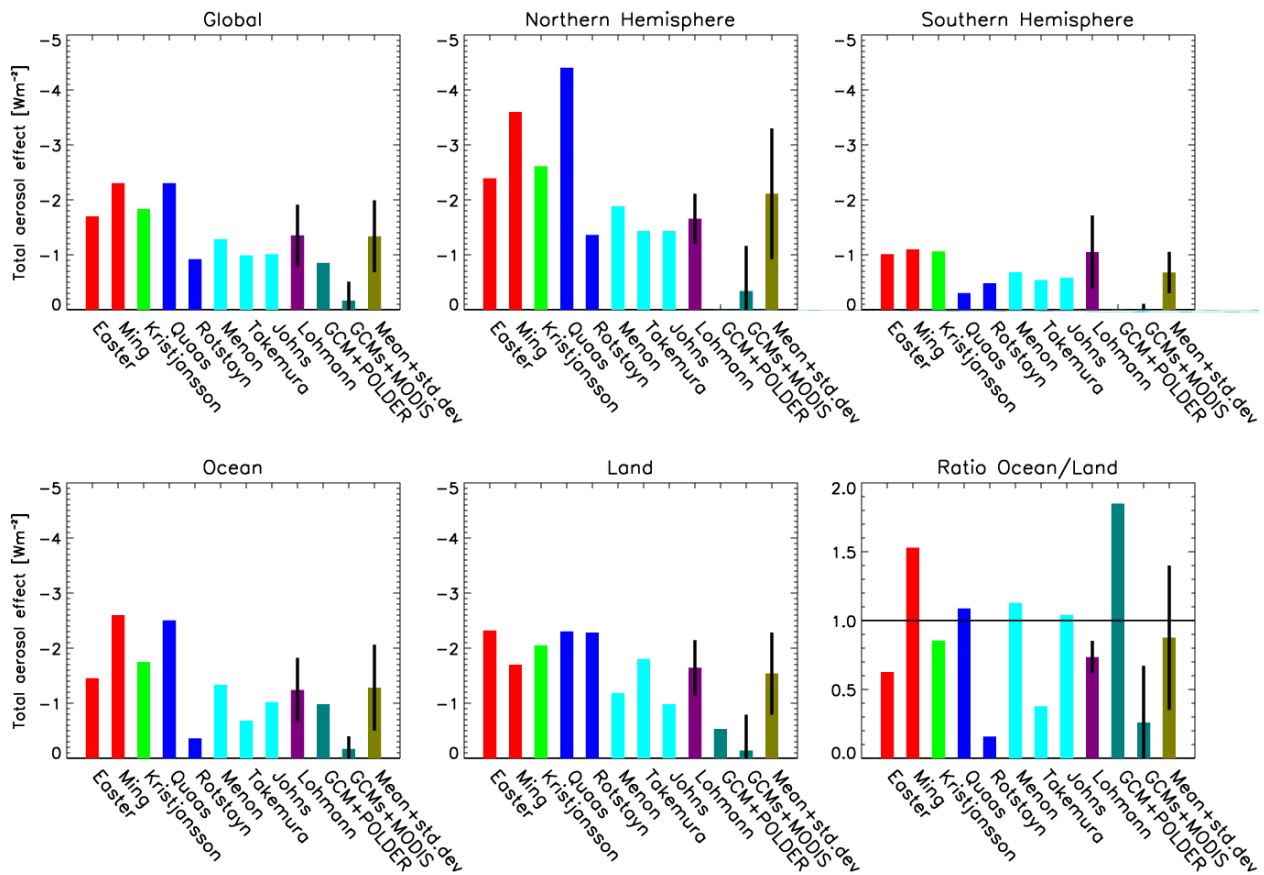
Glaciation effect (positive radiative effect at TOA and more precipitation), thermodynamic effect (sign of radiative effect and change in precipitation not yet known)



3
4
5
6

Figure 7.5.3. Schematic of the aerosol effects discussed in Tables 7.5.1a and 7.5.1b.

1
2



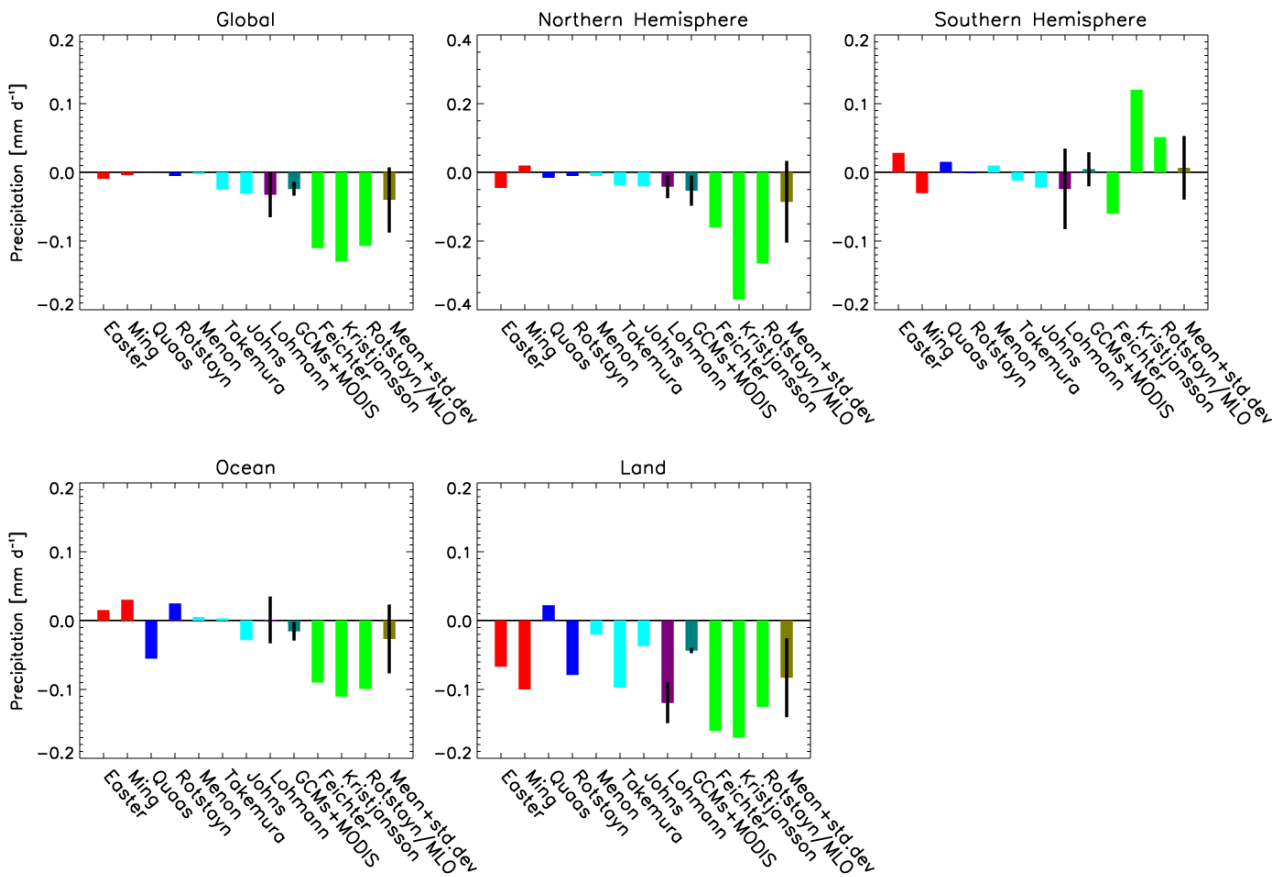
3
4
5
6
7
8
9
10
11
12
13
14
15
16
17
18
19

Figure 7.5.4. Global mean total anthropogenic aerosol effect (direct, semi-direct and indirect cloud albedo and lifetime effects) defined as the response in net radiation at the top-of-the-atmosphere from pre-industrial times to present-day and its contribution over the Northern Hemisphere (NH), Southern Hemisphere (SH), over oceans and over land, and the ratio over oceans/land. Red bars refer to anthropogenic sulphate (Easter et al., 2004; Ming et al., 2005⁺), green bars refer to anthropogenic sulphate and black carbon (Kristjánsson, 2002^{*,+}), blue bars to anthropogenic sulphate and organic carbon (Quas et al., 2004^{*,+}; Rotstajn and Liu, 2005⁺), turquoise bars to anthropogenic sulphate, black, and organic carbon (Menon and Del Genio, 2005; Takemura et al., 2005; Johns et al., 2006), dark purple bars to the mean and standard deviations of anthropogenic sulphate, black, and organic carbon effects on water and ice clouds (Lohmann and Diehl, 2006), teal bars refer to a combination of GCM and satellite results (ECHAM+POLDER, Lohmann and Lesins, 2002; LMDZ/ECHAM+MODIS, Quas et al., 2005) and olive bars to the mean plus standard deviation from all simulations.

*refers to estimates of the aerosol effect deduced from the shortwave radiative flux only

+ refers to estimates solely from the indirect effects

1
2

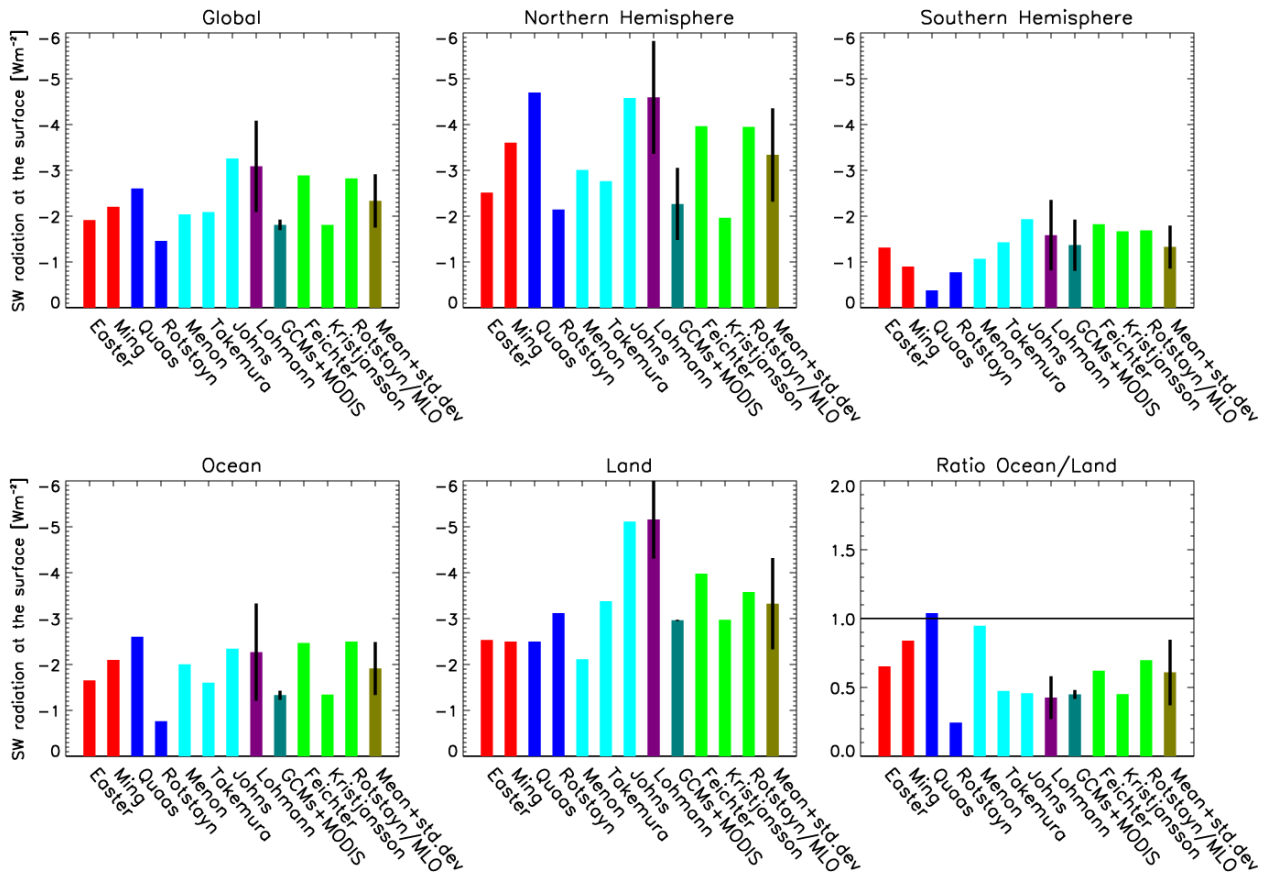


3
4
5
6
7
8
9
10
11
12
13
14
15
16
17
18
19

Figure 7.5.5. Global mean change in precipitation due to the total anthropogenic aerosol effect (direct, semi-direct and indirect cloud albedo and lifetime effects) from pre-industrial times to present-day and its contribution over the Northern Hemisphere (NH), Southern Hemisphere (SH) and over oceans and over land. Red bars refer to anthropogenic sulphate (Easter et al., 2004; Ming et al., 2005⁺), blue bars to anthropogenic sulphate and organic carbon (Quaa et al., 2004⁺; Rotstayn and Liu, 2005⁺), turquoise bars to anthropogenic sulphate, black, and organic carbon (Menon and Del Genio, 2005; Takemura et al., 2005; Johns et al., 2006), dark purple bars to the mean and standard deviations of anthropogenic sulphate, black, and organic carbon effects on water and ice clouds (Lohmann and Diehl, 2006), teal bars refer to a combination of GCM and satellite results (LMDZ/ECHAM+MODIS, Quaa et al., 2005), green bars refer to results from coupled atmosphere/mixed-layer ocean (MLO) experiments (Feichter et al., 2004 - sulphate, black, and organic carbon; Kristjansson et al., 2005 - sulphate and black carbon; Rotstayn and Lohmann, 2002⁺ - sulphate only) and olive bars to the mean plus standard deviation from all simulations.

⁺ refers to estimates solely from the indirect effects

1
2



3
4 **Figure 7.5.6.** Global mean change in net solar radiation at the surface due to the total anthropogenic aerosol
5 effect (direct, semi-direct and indirect cloud albedo and lifetime effects) from pre-industrial times to present-
6 day and its contribution over the Northern Hemisphere (NH), Southern Hemisphere (SH), over oceans and
7 over land, and the ratio over oceans/land. Red bars refer to anthropogenic sulphate (Easter et al., 2004; Ming
8 et al., 2005⁺), blue bars to anthropogenic sulphate and organic carbon (Quaas et al., 2004⁺; Rotstayn and Liu,
9 2005⁺), turquoise bars to anthropogenic sulphate, black, and organic carbon (Menon and Del Genio, 2005;
10 Takemura et al., 2005; Johns et al., 2006), dark purple bars to the mean and standard deviations of
11 anthropogenic sulphate, black, and organic carbon effects on water and ice clouds (Lohmann and Diehl,
12 2006), teal bars refer to a combination of GCM and satellite results (LMDZ/ECHAM+MODIS, Quaas et al.,
13 2005), green bars refer to results from coupled atmosphere/mixed-layer ocean (MLO) experiments (Feichter
14 et al., 2004 - sulphate, black, and organic carbon; Kristjansson et al., 2005 - sulphate and black carbon;
15 Rotstayn and Lohmann, 2002⁺ - sulphate only) and olive bars to the mean plus standard deviation from all
16 simulations.

17
18 ⁺ refers to estimates solely from the indirect effects
19

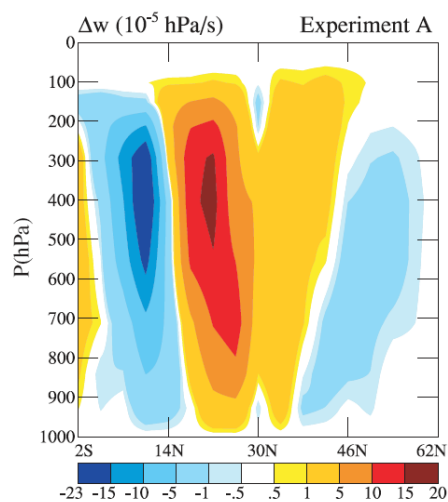
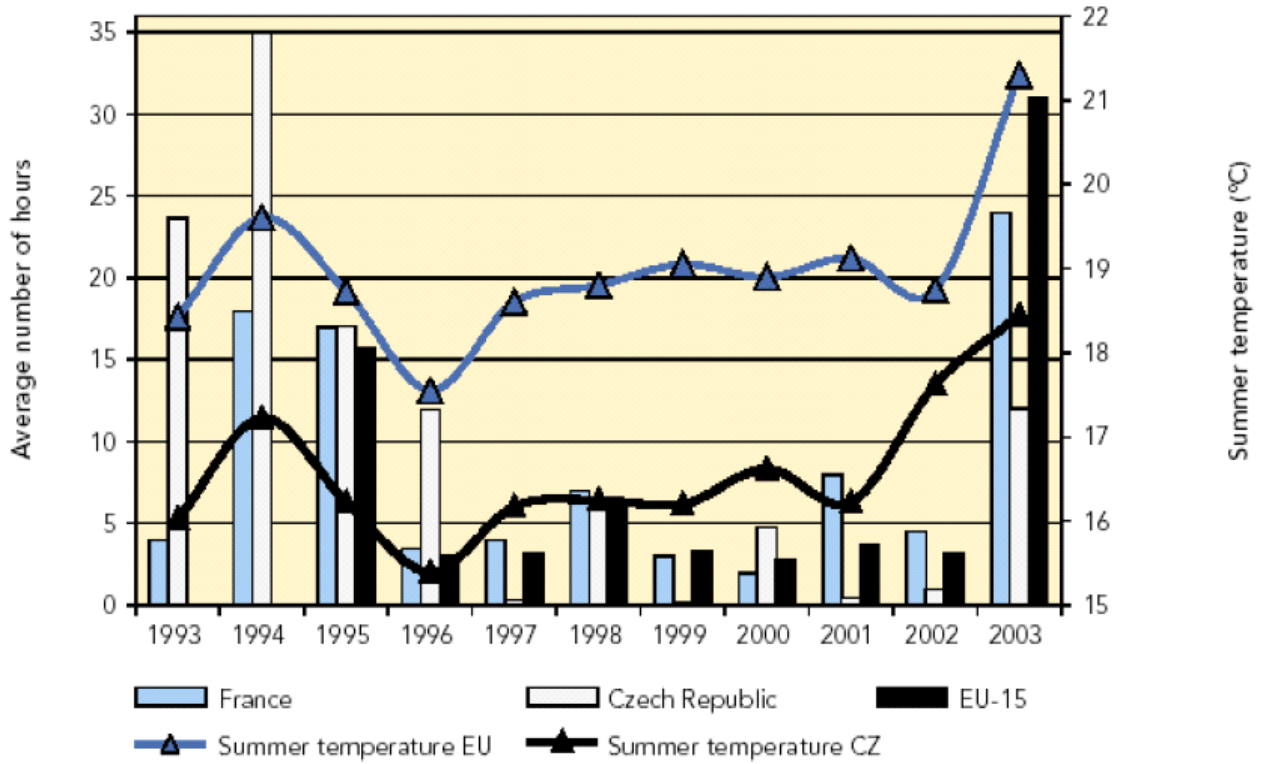
1
23
4
5
6
7
8

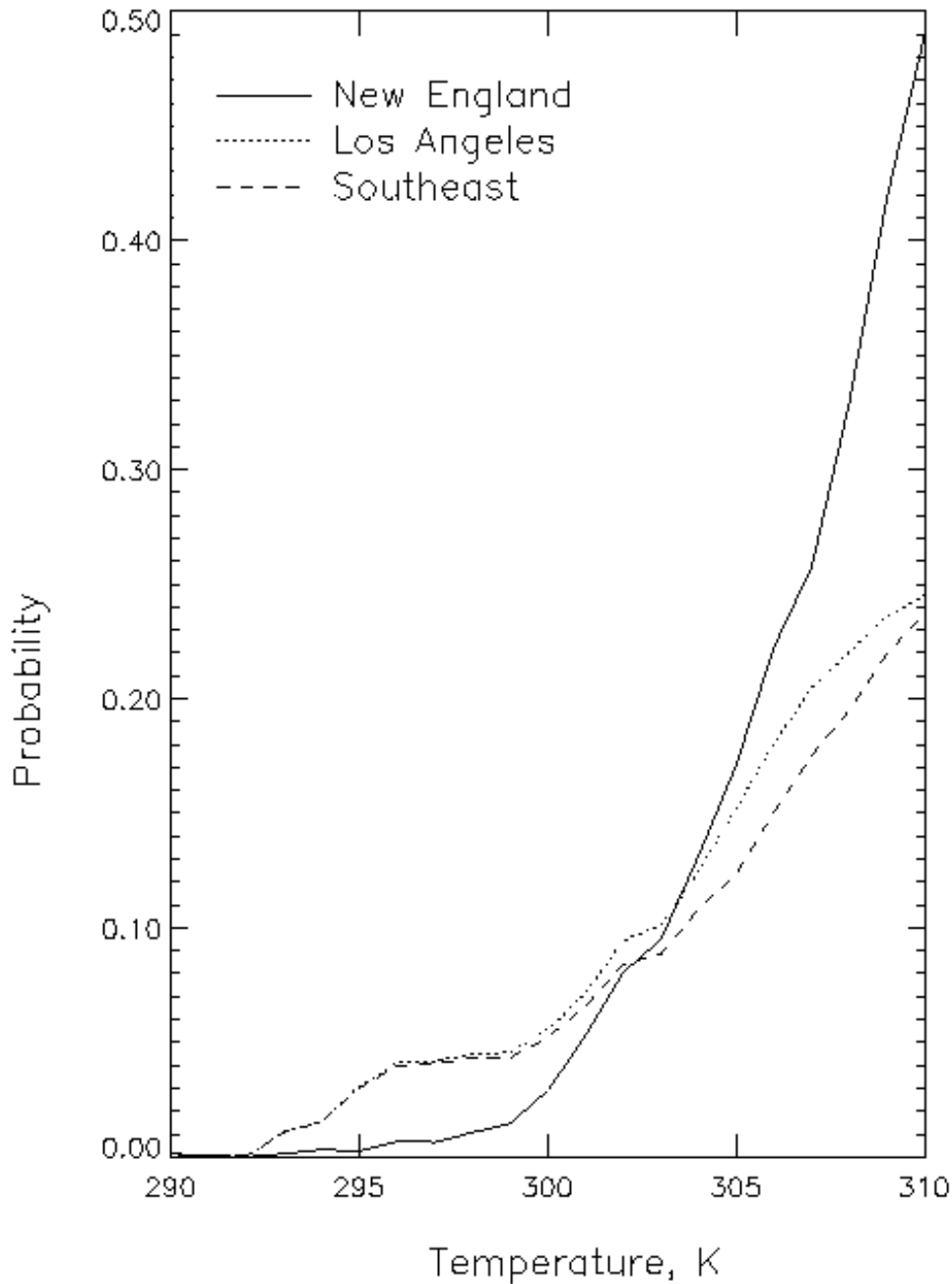
Figure 7.5.7. Simulated (GISS GCM) JJA vertical velocity change as a function latitude and altitude averaged over 90°E to 130°E for the experiment with aerosols representative of the measurements made over the Indian Ocean region and industrial regions of China (With courtesy from Menon et al., 2002b).

1
2



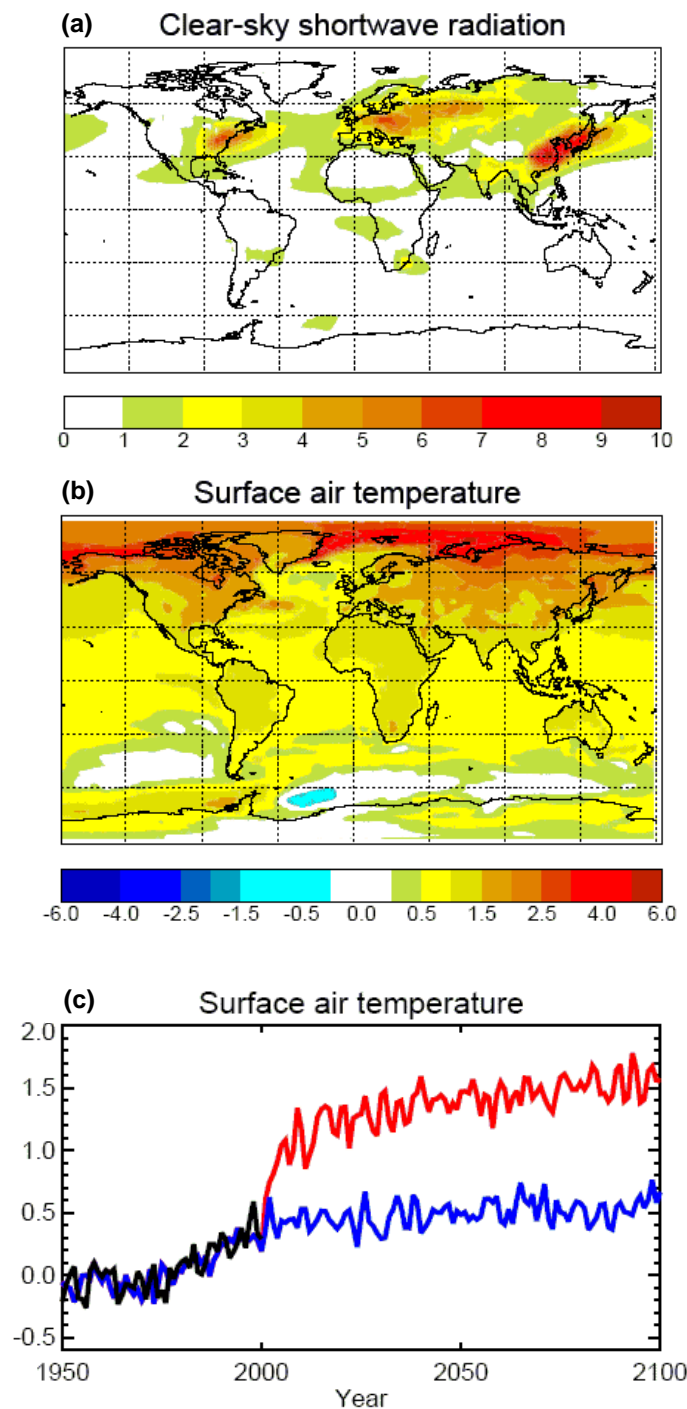
3
4
5
6
7
8

Box 7.4, Figure 1. Average number of hours with ozone concentrations exceeding $180 \mu\text{g}^3$ in France, the Czech Republic (CZ), and the European Union for the period 1993–2003, illustrating the strong link with temperature. From Science Panel on Atmospheric Research (2005).



1
2
3
4
5
6
7
8

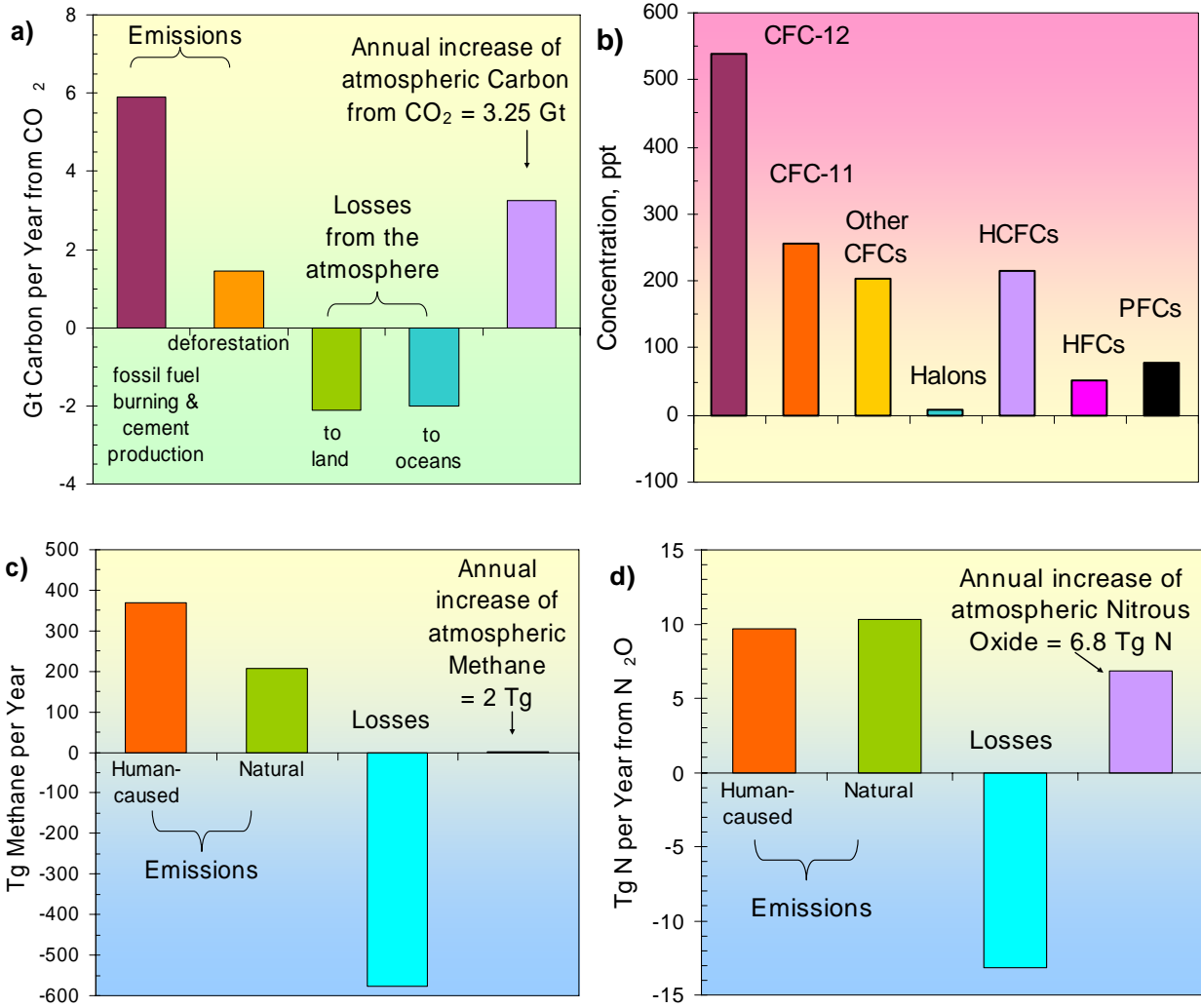
Box 7.4, Figure 2. Probability that the daily maximum 8-hour average ozone will exceed the U.S. National Ambient Air Quality Standard (NAQS) of 0.08 ppmv for a given daily maximum temperature, based on 1980-1998 data. Values are shown for New England (bounded by 36°N, 44°N, 67.5°W, and 87.5°W), the Los Angeles Basin (bounded by 32°N, 40°N, 112.5°W, and 122.5°W) and the southeastern United States (bounded by 32°N, 36°N, 72.5°W, and 92.5°W). From Lin et al. (2001).

1
2

3
4
5 **Figure 7.6.1.** Effect of removing the entire burden of sulphate aerosols in year 2000 on (upper panel) the
6 annual mean clear-sky top of the atmosphere shortwave radiation (W m^{-2}) calculated by Brasseur and
7 Roeckner (2005) for the time period 2071–2100, and (middle panel) on the annual mean surface air
8 temperature ($^{\circ}\text{C}$) calculated for the same time period. Lower panel: temporal evolution of global and annual
9 mean surface air temperature anomalies ($^{\circ}\text{C}$) with respect to the mean 1961–1990 values. The evolution
10 prior to year 2000 is driven by observed atmospheric concentrations of greenhouse gases and aerosols as
11 adopted by IPCC (see Chapter 10). For years after 2000, the concentration of greenhouse gases remains
12 constant while the aerosol burden is unchanged (blue line) or set to zero (red line). The black curve shows
13 observations (Jones et al., 2001: Global and hemispheric temperature anomalies 1856–2000 – land and
14 marine instrumental records. <http://cdiac.ornl.gov/trends/temp/jonescru/jones.html>).

15

1
2
3
4
5
6
7
8
9
10
11
12
13
14
15
16
17
18
19
20
21
22
23
24
25
26
27
28
29
30
31
32
33
34
35
36
37
38
39
40
41
42
43
44
45
46
47
48
49
50
51
52
53
54
55
56
57



Question 7.1, Figure 1. Breakdown of contributions to the changes in atmospheric greenhouse-gas concentrations. This Figure is based on information detailed in Chapters 4 and 7. (a) Contributions to atmospheric carbon dioxide (CO₂) for 1980–2000. Each year carbon dioxide is released to the atmosphere by human activities including fossil fuel combustion and land use change. Only 57-60 % of the carbon dioxide emitted from human activity remains in the atmosphere. Some is dissolved into the oceans and some is incorporated into plants as they grow. 1 Gt = 10¹⁵g (1 billion metric tonnes). (b) Atmospheric concentrations

1 in 2003 of CFCs and other halogen-containing compounds. These chemicals are almost exclusively human-
2 produced. (About one-half of the most abundant perfluorocarbon (PFC) CF_4 is naturally produced.) 1 ppt = 1
3 part in 10^{12} . (c) Sources and sinks of methane (CH_4). Anthropogenic or human-caused sources of methane
4 include energy production, land fills, ruminant animals (e.g. cattle and sheep), rice agriculture and biomass
5 burning. 1 Tg = 10^{12} g (1 million metric tonnes). (d) As (c), but for nitrous oxide (N_2O). Anthropogenic or
6 human-caused sources of N_2O include the transformation of fertilizer N into N_2O and its subsequent
7 emission from agricultural soils, biomass burning, cattle, and some industrial activities including nylon
8 manufacture. (e) Tropospheric ozone. The increase in tropospheric ozone since preindustrial times is a result
9 of chemical reactions of tropospheric pollutants emitted from human activities such as burning of fossil or
10 forest fuels. Tropospheric ozone is short-lived, being destroyed on timescales of days to weeks, thus its
11 concentrations are highly variable.

12
13
14